Supplementary Information

Transformative Binder-Free Strategy Shatters Cyclability Limits for High-Energy Density Oxide Anode-Based Lithium-Ion Batteries

*Abhinav Tandon and Yogesh Sharma**

Abhinav Tandon 1
Department of Physics
IIT Roorkee, Roorkee - 247667
Uttarakhand, India

Yogesh Sharma 2
Department of Physics & Center for Sustainable Energy
IIT Roorkee, Roorkee - 247667
Uttarakhand, India
E-mail: yogesh.sharma@ph.iitr.ac.in

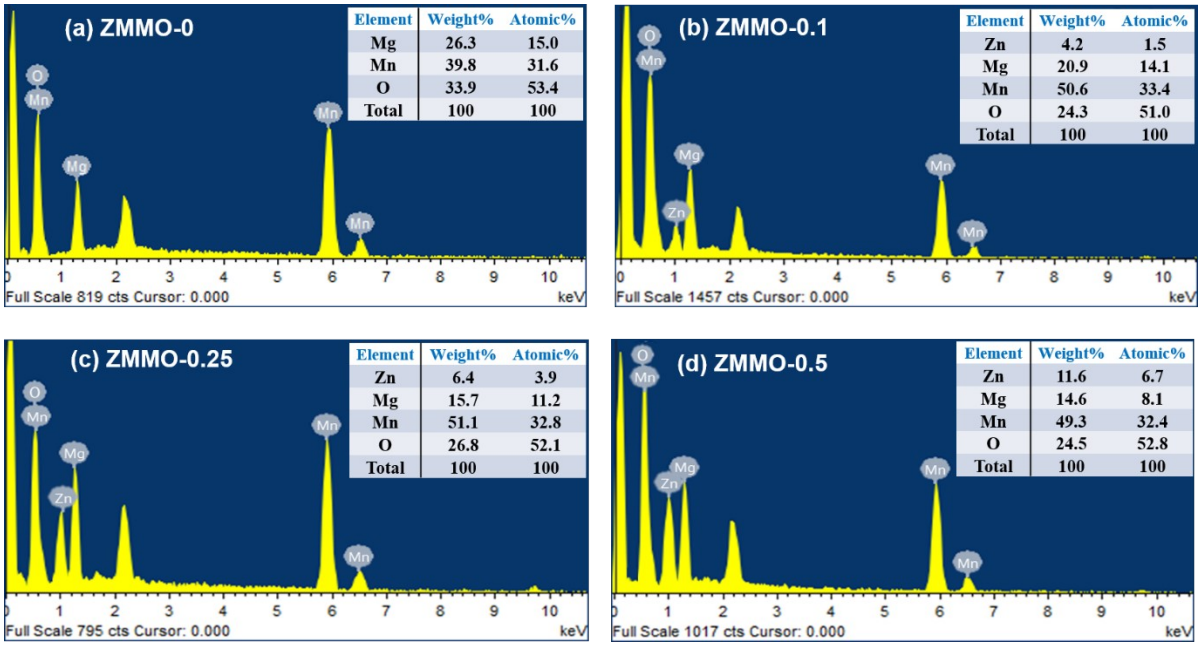

Fig. S1. EDX of $Zn_xMg_{1-x}Mn_2O_4$ (x = 0, 0.1, 0.25, and 0.5) nanofibers.

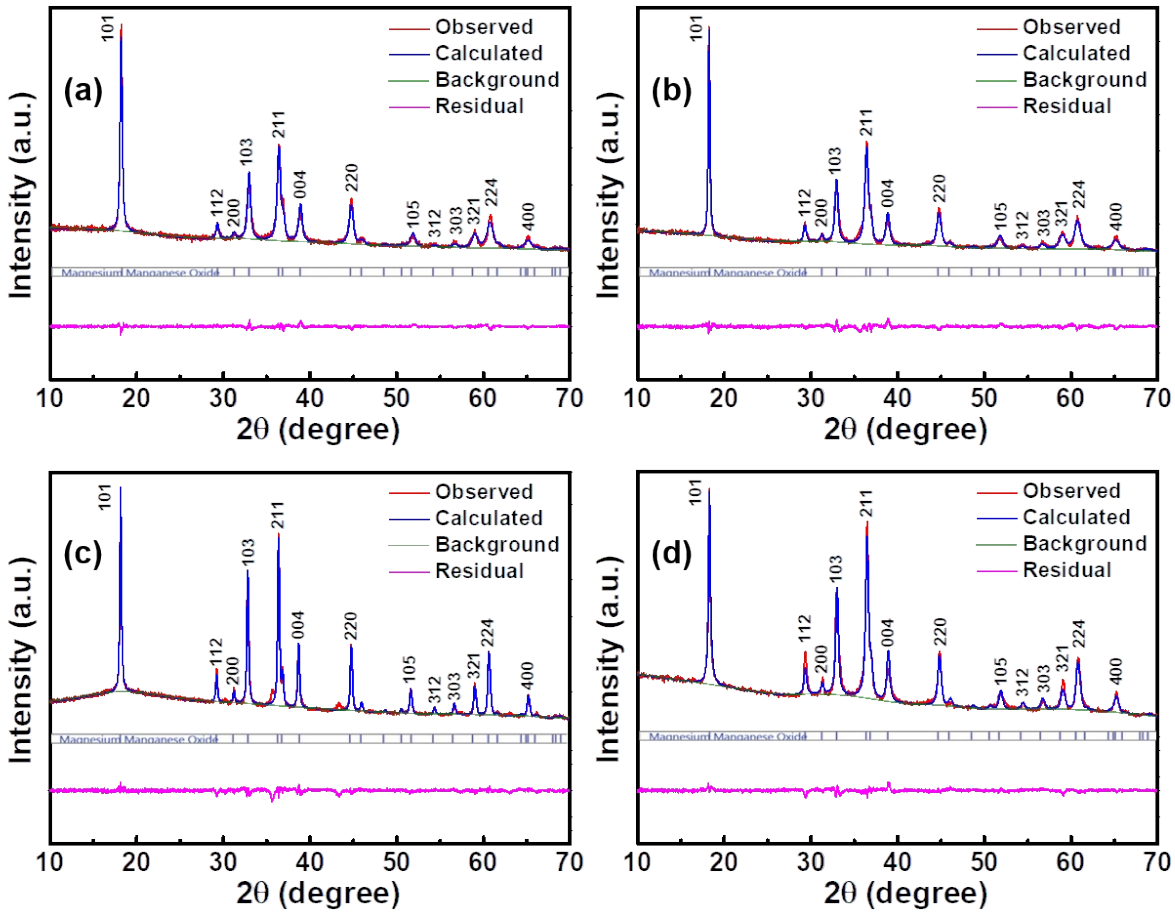

Fig. S2. Rietveld refined XRD patterns of (a) ZMMO-0, (b) ZMMO-0.1, (c) ZMMO-0.25 and (d) ZMMO-0.5.

Table S1. Refined crystallographic parameters of ZMMO-0 sample: a = b = 5.7317(14) Å, c = 9.255(2) Å, χ^2: 2.16, *S*: 1.47, R_p (%): 4.63, R_{wp} (%): 6.26, and R_{exp} (%): 4.25.

Elements	*x*	*y*	*z*	Occupancy
O	0.000000	0.5144(8)	0.2392(4)	1.000
Mn	0.000000	0.000000	0.000000	1.000
Mg	0.000000	0.250000	0.375000	1.000

Table S2. Refined crystallographic parameters of ZMMO-0.1 sample: a = b = 5.731(16) Å, c = 9.276(13) Å, χ^2: 2.26, *S*: 1.50, R_p (%): 5.18, R_{wp} (%): 6.91, and R_{exp} (%): 4.59.

Elements	*x*	*y*	*z*	Occupancy
O	0.000000	0.5013(10)	0.2458(6)	1.000
Mn	0.000000	0.000000	0.000000	1.000
Mg	0.000000	0.250000	0.375000	1.000

Table S3. Refined crystallographic parameters of ZMMO-0.25 sample: a = b = 5.734(10) Å, c = 9.283(15) Å, χ^2: 2.09, *S*: 1.44, R_p (%): 5.29, R_{wp} (%): 6.98, and R_{exp} (%): 4.82.

Elements	*x*	*y*	*z*	Occupancy
O	0.000000	0.5131(7)	0.2381(4)	1.000
Mn	0.000000	0.000000	0.000000	1.000
Mg	0.000000	0.250000	0.375000	1.000

Table S4. Refined crystallographic parameters of ZMMO-0.5 sample: a = b = 5.738(6) Å, c = 9.297(10) Å, χ^2: 2.42, *S*: 1.55, R_p (%): 3.93, R_{wp} (%): 5.54, and R_{exp} (%): 3.56.

Elements	*x*	*y*	*z*	Occupancy
O	0.000000	0.5145(6)	0.2478(3)	1.000
Mn	0.000000	0.000000	0.000000	1.000
Mg	0.000000	0.250000	0.375000	1.000

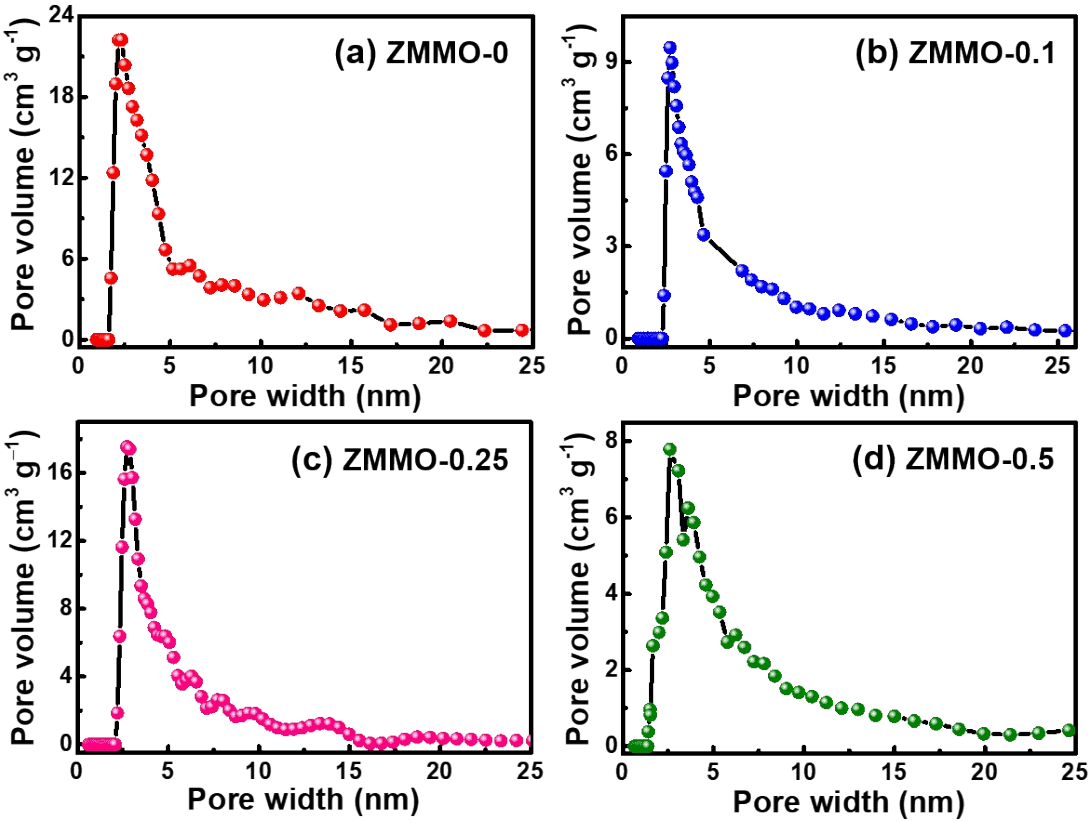

Fig. S3. Pore size distribution (PSD) of $Zn_xMg_{1-x}Mn_2O_4$ (x = 0, 0.1, 0.25, and 0.5) nanofibers.

Table S5. Findings of N_2 adsorption/desorption isotherm analyses.

Material	Specific surface area (m^2 g^{-1})	Total pore volume (cc/g)	Average pore size (nm)
ZMMO-0	70	0.094	2.335
ZMMO-0.1	74	0.047	2.735
ZMMO-0.25	68	0.043	2.604
ZMMO-0.5	63	0.044	2.712

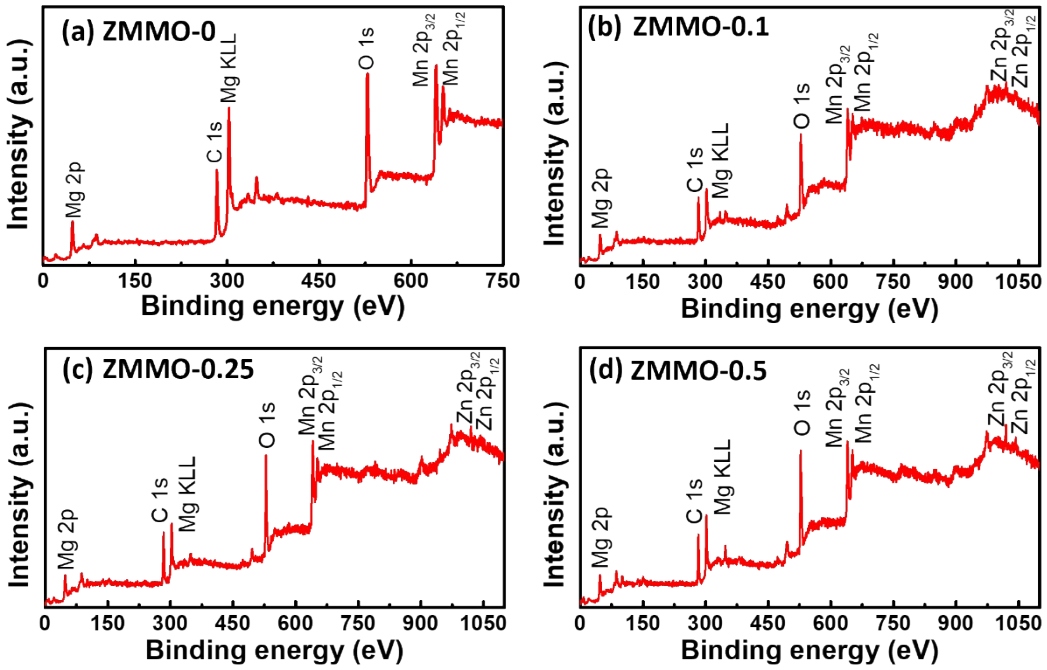

Fig. S4. XPS survey spectrum of (a) ZMMO-0, (b) ZMMO-0.1, (c) ZMMO-0.25, and (d) ZMMO-0.5 nanofibers.

The Mg 2p high-resolution XPS spectra for the ZMMO nanofiber samples, shown in Fig. S5a-d, indicate the presence of Mg^{2+} ions around 50.92 eV.[1,2] Similarly, Fig. S5e-h presents the high-resolution Mn 2p spectra for the fabricated samples. These spectra display two spin-orbit doublets, with Mn $2p_{1/2}$ at 653.33 eV and Mn $2p_{3/2}$ at 641.77 eV, separated by a spin-orbit splitting of approximately 11.56 eV. In the Gaussian-fitted Mn 2p spectra, the peaks were attributed to Mn^{3+} (641.2, 652.6 eV) and Mn^{2+} (642.5, 654.1 eV) oxidation states, respectively.[3,4] High-resolution O 1s XPS spectra for all as-fabricated samples, as illustrated in Fig. S5i-l, reveal three distinct peaks. The peaks at binding energies of 529.54 and 531.70 eV correspond to lattice oxygen (O_L) and vacancy sites/oxygen defects (O_d), respectively. The third peak, observed at 533.34 eV, is associated with oxygen atoms in surface-adsorbed water molecules (O_W).[5,6] In the Zn 2p spectrum shown in Fig. S5(m-o), two peaks appear at binding energies of 1020.65 eV and 1043.92 eV, which are attributed to Zn $2p_{3/2}$ and Zn $2p_{1/2}$, respectively. This peak separation of approximately 23 eV confirms the oxidation state of Zn

in the ZMMO. This binding energy difference aligns well with reported values for Zn^{2+} species.[7,8] Collectively, these XPS findings support the successful formation of pure-phase ZMMO nanofibers.

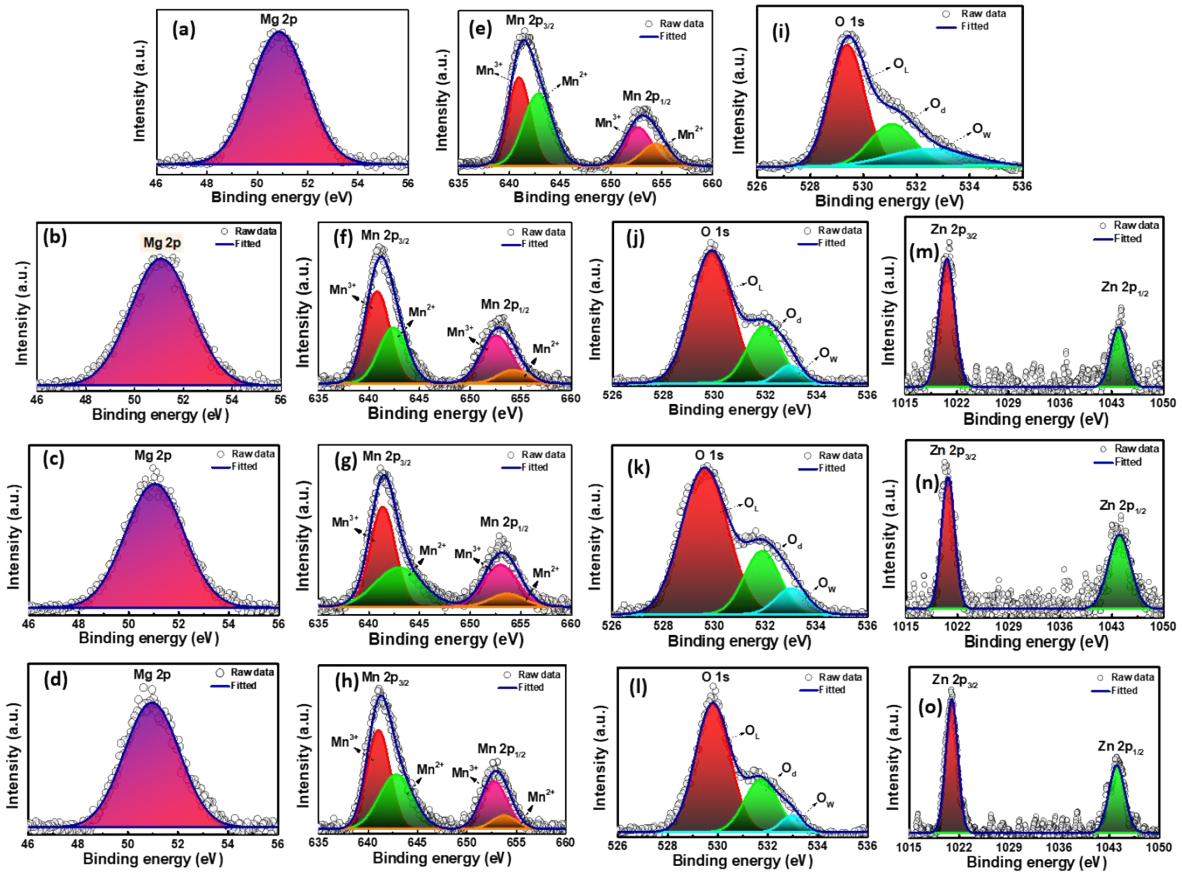

Fig. S5. High-resolution XPS spectra of (a-d) Mg 2p, (e-h) Mn 2p, (i-l) O 1s, and (m-o) Zn 2p of ZMMO-0, ZMMO-0.1, ZMMO-0.25, and ZMMO-0.5 nanofibers, respectively.

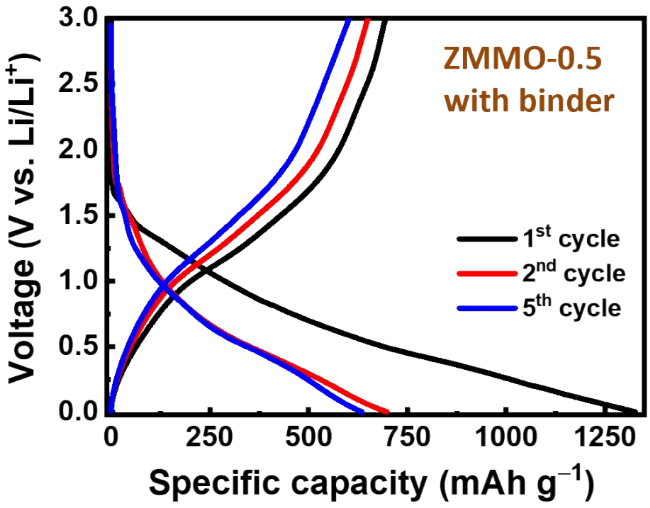

Fig. S6. GCD curves of the ZMMO-0.5 nanofiber electrode prepared via a conventional slurry-coating method with a binder.

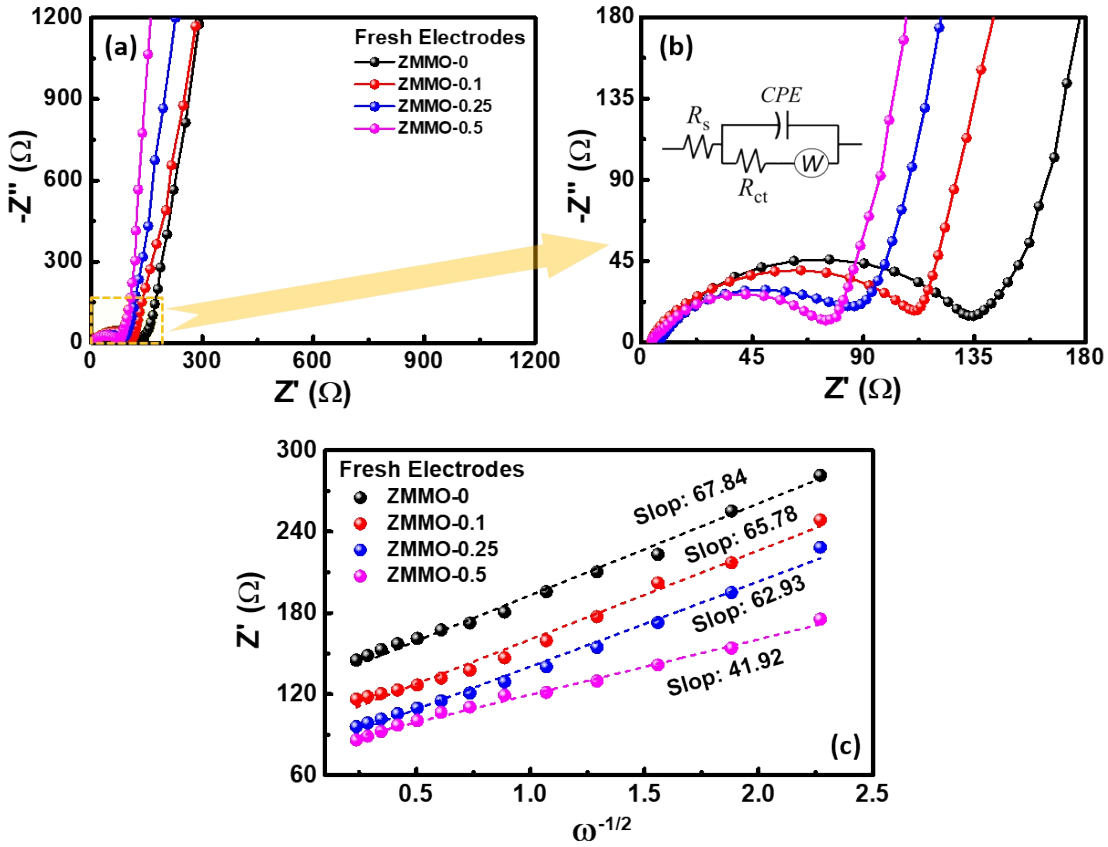

Fig. S7. (a) Nyquist plots, (b) zoomed-in Nyquist plots, and (c) linear fitting relationships of the $Z' - \omega^{-1/2}$ plots of ZMMO-0, ZMMO-0.1, ZMMO-0.25, and ZMMO-0.5 fresh electrodes.

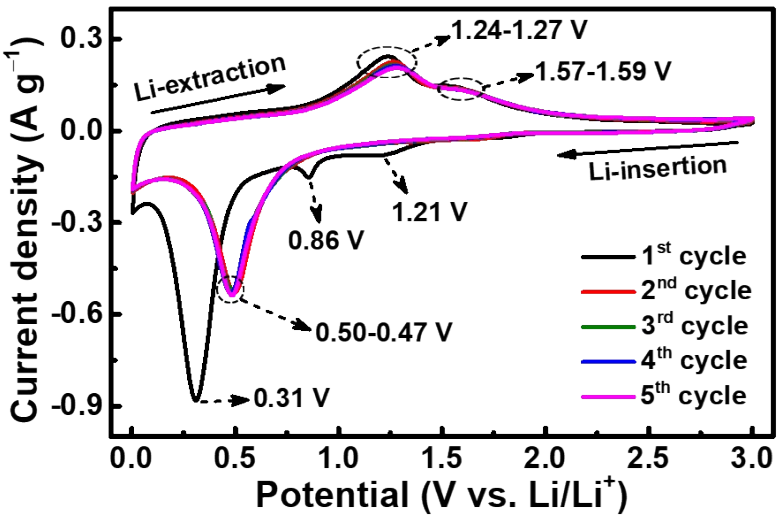

Fig. S8. Cyclic voltammetry of ZMMO-0.5 nanofibers electrode at 0.1 mV s^{-1} scan rate.

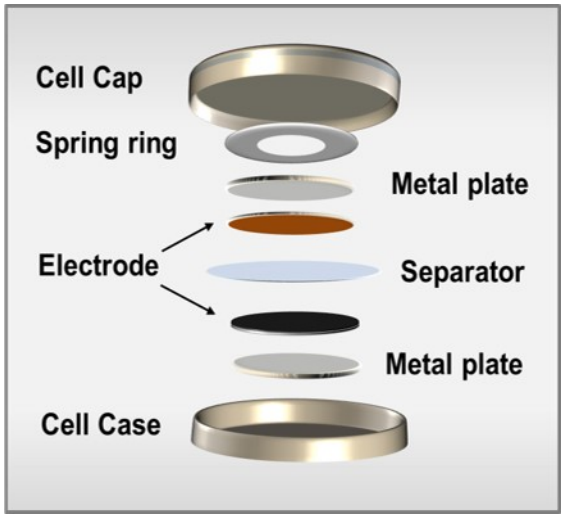

Fig. S9. Schematic illustration of full-cell assembly steps.

Table S6: Comparative Performance of ZMMO-0.5 Electrode with Literature Data.

Material composition	Li-storage characteristics [capacity (mAh g^{-1}) @no. of cycles @current density]	Rate performance (mAh g^{-1})	Ref.
N–doped carbon encapsulated Mn_2O_3/MnO	683.6 @1000 @0.5 A g^{-1}	660 @1.6 A g^{-1}	9
Mn_xO_y-derived metal-organic frameworks	520 @70 @0.1 A g^{-1}	441 @1 A g^{-1}	10
Mn_2O_3 nanoparticles embedded into N–doped carbon	559 @500 @0.5 A g^{-1}	520 @1.2 A g^{-1}	11
β-$Mn_2V_2O_7$ nanorods	253 @100 @0.5 A g^{-1}	222 @2.5 A g^{-1}	12
Mn_3O_4 NRs/rGO	669 @100 @0.1 A g^{-1}	-	13
$ZnMn_2O_4$–rGO/CNTs	606 @1000 @1 A g^{-1}	94 @5 A g^{-1}	14
MnO@Mn_2O_3 nanocrystals embedded in biochar	446.9 @200 @0.5 A g^{-1}	@2 A g^{-1}	15
$CuMn_2O_4$/graphene nanosheets	935 @150 @0.05 A g^{-1}	478 @1 A g^{-1}	16
Graphene coated core-shell Mn_3O_4 nanoparticles	353 @50 @0.1 A g^{-1}	374 @0.5 A g^{-1}	17
$CoMn_2O_4$ microflowers	650 @500 @1 A g^{-1}	257 @2 A g^{-1}	18
$Zn_{0.5}Mg_{0.5}Mn_2O_4$ nanofibers (ZMMO-0.5)	874 @400 @1 A g^{-1} 186 @2000 @2.5 A g^{-1}	108 @5 A g^{-1}	This work

Table S7: Electrode parameters and calculated cell metrics of the NCM//ZMMO-0.5 full cell.

Cell Parameter	Values	
	ZMMO-0.5 Anode	NCM Cathode
Mass loading (mg cm^{-2})	0.25	1.5
Total electrode mass (mg)	0.50	3.00
Coating thickness (μm)	12	30
True density (g cm^{-3})	4.494	4.587
Compaction density (g cm^{-3})	0.208	0.50
Theoretical porosity (%)	95.4	89.1
Pore volume (cm^3)	0.00229	0.00534
Electrolyte absorbed (mg)	4.126	9.623
Separator dry mass (mg)	2.86	
Separator electrolyte (mg)	5.218	
Total electrolyte mass (mg)	18.97	
Cu current collector (mg)	17.44	
Al current collector (mg)	8.43	
Total cell mass (mg)	51.20	
Average working voltage (V)	2.54	
Discharge capacity (mAh)	0.313	
Cell energy (mWh)	0.795	

References

1. X. Wang, G. Zhai and H. Wang, *J Nanopart Res*, 2015, **17**, 339.
2. W. N. R. W. Isahak, S. Z. Hasan, Z. A. C. Ramli, M. M. Ba-Abbad and M. A. Yarmo, *Res Chem Intermed*, 2019, **45**, 951–953.
3. C. Si, J. Zhang, Y. Wang, W. Ma, H. Gao, L. Lv and Z. Zhang, *ACS Appl. Mater. Interfaces*, 2017, **9**, 2485–2494.
4. B. Pattanayak, F. M. Simanjuntak, D. Panda, C.-C. Yang, A. Kumar, P. – A. Le, K. – H. Wei and T. –Yuen Tseng, *Sci Rep*, 2019, **9**, 16852.
5. J. J. William, I. M. Babu and G. Muralidharan, *New J. Chem.*, 2019, **43**, 15375–15388.
6. Z.-F. Huang, S. Xi, J. Song, S. Dou, X. Li, Y. Du, C. Diao, Z. J. Xu and X. Wang, *Nat Commun*, 2021, **12**, 3992.
7. Y. Wang, S. Xu, Y. Zhang, L. Hou and C. Yuan, *Nanomaterials*, 2023, **13**, 512.
8. J. Chen, H. Zuo, C. Wang, Y.-C. Zhang, W. Gao, N. Zhao, Y. Huang and S. Xiao, *Electrochimica Acta*, 2022, **426**, 140780.
9. X. Liu, Y. Liu, M. Jin, C. Xu, Y. Tian, M. Zhou, W. Wang, G. Li, Z. Hou and L. Chen, *Journal of Colloid and Interface Science*, 2024, **665**, 752–763.
10. T. B. N. Le, H. T. Lai, T. L. Nguyen, Q. N. Tran, N. Q. M. Tran, L. H. T. Nguyen, T. L. H. Doan, A. T. T. Pham, C. K. Jayasankar, B. Jang, J. Hong and T. B. Phan, *Solid State Sciences*, 2024, **151**, 107504.
11. L. Chen, Y. Liu, L. Yang, C. Xu, W. Wang, G. Li, Y. Zhu, M. Zhou and Z. Hou, *Chemical Engineering Science*, 2024, **285**, 119626.
12. T. L. Soundarya, M. Jayachandran, T. Maiyalagan, B. Nirmala, G. Nagaraju and H. N. Anil Rao, *Journal of Energy Storage*, 2024, **85**, 111076.
13. Y. Liu, W. Wang, Y. Wang, Y. Ying, L. Sun and X. Peng, *RSC Adv.*, 2014, **4**, 16374.
14. Q. Tang, Y. Shi, Z. Ding, T. Wu, J. Wu, V. Mattick, Q. Yuan, H. Yu and K. Huang, *Electrochimica Acta*, 2020, **338**, 135853.
15. Y. Li, X. Xu, Y. Tang, Y. Sima, J. Yang, P. Lu, X. Liu, S. Xu, W. Yin, J. Zhao, S. Shi, H. Ji, Z. Chen and G. Yang, *Surfaces and Interfaces*, 2024, **49**, 104424.
16. L. Li, G. Jiang and J. Ma, *Materials Research Bulletin*, 2018, **104**, 53–59.
17. Thauer, X. Shi, S. Zhang, X. Chen, L. Deeg, R. Klingeler, K. Wenelska and E. Mijowska, *Energy*, 2021, **217**, 119399.
18. L. Zhang, G. He, S. Lei, G. Qi, H. Jiu and J. Wang, *Journal of Power Sources*, 2016, **326**, 505–513.